Materials for Quantum Technology

Dynamic Brillouin cooling for continuous optomechanical systems

IOP Publishing Mater. Quantum Technol. 3 (2023) 015003 https://doi.org/10.1088/2633-4356/acc2a5

Materials for Quantum Technology

OPEN ACCESS

RECEIVED
12 December 2022

REVISED
21 February 2023

ACCEPTED FOR PUBLICATION
8 March 2023

PUBLISHED
22 March 2023

PAPER

Dynamic Brillouin cooling for continuous optomechanical systems

Changlong Zhu[1,2,*] and **Birgit Stiller**[1,2,*]

[1] Max Planck Institute for the Science of Light, Staudtstr. 2, 91058 Erlangen, Germany
[2] Department of Physics, University of Erlangen–Nuremberg, Staudtstr. 7, 91058 Erlangen, Germany
[*] Authors to whom any correspondence should be addressed.

E-mail: changlong.zhu@mpl.mpg.de and birgit.stiller@mpl.mpg.de

Keywords: mechanical cooling, Brillouin scattering, quantum optics, optomechanics

Supplementary material for this article is available online

Abstract

Up until now, ground state cooling using optomechanical interaction is realized in the regime where optical dissipation is higher than mechanical dissipation. Here, we demonstrate that optomechanical ground state cooling in a continuous optomechanical system is possible by using backward Brillouin scattering while mechanical dissipation exceeds optical dissipation which is the common case in optical waveguides. The cooling is achieved in an anti-Stokes backward Brillouin process by modulating the intensity of the optomechanical coupling via a pulsed pump to suppress heating processes in the strong coupling regime. With such dynamic modulation, a significant cooling factor can be achieved, which can be several orders of magnitude lower than for the steady-state case. This modulation scheme can also be applied to Brillouin cooling generated by forward intermodal Brillouin scattering.

1. Introduction

Cooling a mechanical oscillator to its ground state by overcoming the effects of thermal environment has always attracted great interest, as it offers attractive opportunities for various topics including high precision metrology [1–3], quantum information processing [4–6], and the exploration of classical-and-quantum limit of macroscopic objects [7–9]. Preparing a single mode mechanical oscillator into its quantum ground state has been experimentally realized in cavity optomechanical systems [10] by utilizing the technique of sideband cooling [11–14], which plays a central role in a host of novel quantum technologies, ranging from generation of nonclassical states [15–17] to quantum sensors [18] and quantum repeaters [19]. Beyond cooling single mechanical modes in cavity optomechanics, novel cooling technologies, for example, multimode cooling methods by using EIT [20], dark-mode control [21], cold-damping feedback [22–24], synthetic magnetism [25], and quantum reservoir engineering [26], have been developed in recent years for extended platforms with many degrees of freedom, including multiple degenerate mechanical resonators [27–31], optomechanical arrays [32–37], optically levitated mechanical resonators [38, 39], and waveguide-coupled resonators [40, 41]. The intriguing limit of these cases is the ground-state cooling in continuous optomechanical systems [42, 43].

Among the laser cooling techniques that provide refrigeration for gases [44–46] and solids [47–52], Brillouin-based technologies provide cooling for groups of phonons in continuous optomechanical systems [53–55]. Brillouin-based optomechanical continuum cooling, i.e. so-called Brillouin cooling, opens a new avenue to study quantum nonlinear optics [56], quantum computing [57, 58], and quantum networks [59–61] with remarkable optical and mechanical bandwidths. One of the prerequisites for Brillouin cooling is that photons must dissipate more quickly than phonons to prevent energy from reabsorbing or transferring back to phonons [53, 55, 62–64]. This requirement causes limitations to Brillouin cooling. Optomechanical continuum cooling was so far only observed in a state-of-the-art silicon waveguide [55] by utilizing forward intermodal Brillouin scattering recently where photonic dissipation exceeds phononic dissipation, which simply cools a band of acoustic phonons by around 30 K from room temperature. For general backward Brillouin scattering with higher frequency and thus lower Q-factor, it was thought to be

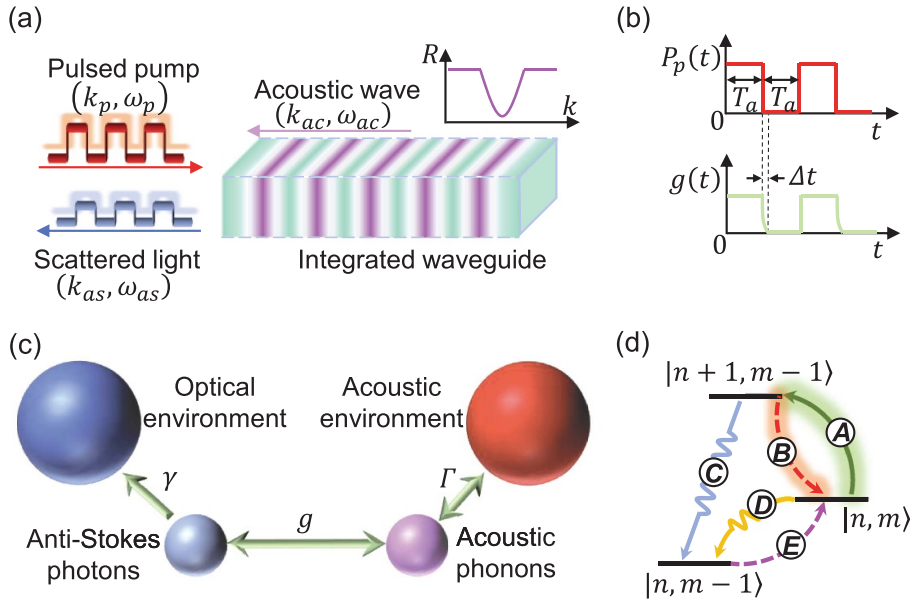

Figure 1. (a) Schematic diagram of the optomechanical continuum cooling via the backward anti-Stokes Brillouin scattering by utilizing a pulsed pump, where R and k indicate the cooling rate and the wavenumber. (b) Modulation of the intensity of the optomechanical coupling strength $g(t)$ via a pulsed laser $P_{\rm p}(t)$ in a short Brillouin-active waveguides, where the time Δt consumed by lights passing through the waveguide is far smaller than the evolution time $T_{\rm a}$ of the system, i.e. $\Delta t \ll T_{\rm a}$. (c) The linearized Brillouin anti-Stokes interaction under the undepleted approximation. (d) Level diagram of the Brillouin cooling in the strong coupling regime where $|n, m\rangle$ denotes the state of n anti-Stokes photons and m acoustic phonons.

impractical for ground-state cooling in continuous optomechanical systems [53, 55]. However, to use continuum systems with their remarkable optical and mechanical bandwidths, it is urgent to overcome these limitations for cooling and manipulating continuous optomechanical systems in the quantum regime.

Recently, a variety of integrated optomechanical waveguides at small size scales (∼cm or mm length) were achieved in experiment [65]. These short Brillouin-active waveguides with high Brillouin gain allow the coherent light–sound interaction in a small regime, which enables the dynamical control of photonic–phononic interaction [66, 67] through a pulsed laser such as coherent photonic–phononic memory [68]. In addition, it has been theoretically predicted that the strong coupling regime of the anti-Stokes Brillouin interaction can be accessible in highly nonlinear waveguides [42, 69]. The strong optomechanical interaction permits state swapping between photons and phonons [70, 71] which is one way to achieve phonon cooling [72–76]. As a consequence, a Brillouin cooling scheme that can beat the phonon heating rate for continuous optomechanical systems coupled with the environment is highly desirable by manipulating the dynamics of photonic–phononic interaction in integrated waveguides.

In this work, we demonstrate that one can achieve a great cooling factor for groups of phonons via backward Brillouin scattering in continuous optomechanical systems under the strong coupling regime, as shown in figure 1(a). By periodically modulating the optomechanical coupling strength through a pulsed laser in a short integrated waveguide, as shown in figure 1(b), the heating generated by the state swapping and thermal noise can be significantly suppressed, which enables the phonon occupancy to reach an instantaneous-state cooling limit and thereby breaks the fundamental limit of Brillouin cooling.

2. Backward Brillouin scattering driven by an undepleted pump

For a typical Brillouin-active waveguide, the backward Brillouin light-scattering is triply resonant where the Stokes and anti-Stokes processes associate with counter-propagating traveling-wave acoustic phonons. This results in a natural dispersive symmetry breaking between the Stokes and anti-Stokes processes [77] and thus enables us to individually study the anti-Stokes process and to explore the optomechanical continuum cooling. Here we consider the backward anti-Stokes Brillouin scattering in a general integrated waveguide. It is a three-wave mixing process between a pump wave $(k_{\rm p}, \omega_{\rm p})$, an anti-Stokes scattered light $(k_{\rm as}, \omega_{\rm as})$, and an acoustic wave $(k_{\rm ac}, \omega_{\rm ac})$, as shown in figure 1(a), where k and ω correspond to wave-vector and frequency, respectively. The phase matching condition and the energy conservation yield requirements:

$$\omega_{\rm ac} = \omega_{\rm as} - \omega_{\rm p}, \quad k_{\rm ac} = k_{\rm as} - k_{\rm p}. \tag{2.1}$$

Under these circumstances, the dynamics of our system driven by a CW laser can be given by [42, 53, 77]

$$\begin{aligned}\frac{\partial a_{\rm p}}{\partial t}+\upsilon_{\rm o}\frac{\partial a_{\rm p}}{\partial z}&=-\frac{\gamma}{2}a_{\rm p}-ig_0b_{\rm ac}^{\dagger}a_{\rm as}+\sqrt{\gamma}\xi_{\rm p},\\ \frac{\partial a_{\rm as}}{\partial t}-\upsilon_{\rm o}\frac{\partial a_{\rm as}}{\partial z}&=-\frac{\gamma}{2}a_{\rm as}-ig_0a_{\rm p}b_{\rm ac}+\sqrt{\gamma}\xi_{\rm as},\\ \frac{\partial b_{\rm ac}}{\partial t}-\upsilon_{\rm ac}\frac{\partial b_{\rm ac}}{\partial z}&=-\frac{\Gamma}{2}b_{\rm ac}-ig_0a_{\rm p}^{\dagger}a_{\rm as}+\sqrt{\Gamma}\xi_{\rm ac},\end{aligned}\tag{2.2}$$

where $a_{\rm p}$, $a_{\rm as}$, and $b_{\rm ac}$ denote the envelope operators of the pump field, scattered anti-Stokes field, and acoustic field, respectively. $\upsilon_{\rm o}$ (γ) and $\upsilon_{\rm ac}$ (Γ) are the group velocities (dissipation rates) of the optical and acoustic fields. g_0 is the traveling-wave vacuum coupling rate which quantifies the interaction intensity between photons and phonons at the single-quanta level. Without loss of generality, we take g_0 real and positive [42]. $\xi_{\rm p}$ ($\xi_{\rm as}$) is the zero-mean quantum Gaussian noise of the pump (anti-Stokes) field. $\xi_{\rm ac}$ represents the thermal noise of the acoustic field which obeys the relations $\langle\xi_{\rm ac}(t,z)\rangle=0$ and $\langle\xi_{\rm ac}^{\dagger}(t_1,z_1)\xi_{\rm ac}(t_2,z_2)\rangle=n_{\rm th}\delta(t_1-t_2)\delta(z_1-z_2)$ [77, 78], where $n_{\rm th}=1/(e^{\hbar\omega_{\rm ac}/k_{\rm B}T_{\rm m}}-1)$ is the thermal phonon occupation at the environment temperature $T_{\rm m}$.

In order to analytically study the dynamics of the nonlinear anti-Stokes process, we consider an undepleted pump [79], which has been extensively used when studying properties of Brillouin scattering processes. Under the undepleted approximation, the three-wave optomechanical interaction can be linearized to an effective optomechanical interaction between the anti-Stokes field and the acoustic field with a pump-enhanced coupling strength $g=g_0\sqrt{\langle a_{\rm p}^{\dagger}a_{\rm p}\rangle}$, as shown in figure 1(c). Thus equation (2.2) can be reduced to [42, 53]

$$\begin{aligned}\frac{\partial a_{\rm as}}{\partial t}-\upsilon_{\rm o}\frac{\partial a_{\rm as}}{\partial z}&=-\frac{\gamma}{2}a_{\rm as}-igb_{\rm ac}+\sqrt{\gamma}\xi_{\rm as},\\ \frac{\partial b_{\rm ac}}{\partial t}-\upsilon_{\rm ac}\frac{\partial b_{\rm ac}}{\partial z}&=-\frac{\Gamma}{2}b_{\rm ac}-iga_{\rm as}+\sqrt{\Gamma}\xi_{\rm ac}.\end{aligned}\tag{2.3}$$

Actually, $a_{\rm as}$ and $b_{\rm ac}$ are modes with a continuous wavenumber and can be expressed as $a_{\rm as}=1/\sqrt{2\pi}\int{\rm d}k\,a_k e^{ikz}$ and $b_{ac}=1/\sqrt{2\pi}\int{\rm d}k\,b_k e^{ikz}$ [77, 80, 81], respectively. Moving to momentum space by replacing $a_{\rm as}$, $b_{\rm ac}$, $\xi_{\rm as}$, $\xi_{\rm ac}$, and $\partial/\partial z$ with a, b, ξ_1, ξ_2, and ik, the dynamics of the linearized anti-Stokes process can be given by

$$\begin{aligned}\dot{a}&=(-\gamma/2+i\Delta_1)\,a-igb+\sqrt{\gamma}\xi_1,\\ \dot{b}&=(-\Gamma/2+i\Delta_2)\,b-iga+\sqrt{\Gamma}\xi_2,\end{aligned}\tag{2.4}$$

where $a(t,k)$ ($b(t,k)$) is the inverse Fourier transform of the envelope operator $a_{\rm as}(t,z)$ ($b_{\rm ac}(t,z)$) and denotes the annihilation operator for the kth photon (phonon) mode, where the subscript k for $a(t,k)$ ($b(t,k)$) has been omitted for simplicity. $\Delta_1=k\upsilon_{\rm as}$ and $\Delta_2=k\upsilon_{\rm ac}$ induced by the wavenumber k are the frequency shifts for the anti-Stokes photons and acoustic phonons. This implies that the Brillouin interaction in a continuous optomechanical system can be treated as a group of channels in the momentum space. Each channel corresponds to an optomechanical interaction for a specific wavenumber k between the pump mode, a scattered optical mode with frequency shift Δ_1 to $\omega_{\rm ac}$, and an acoustic mode with frequency shift Δ_2 to $\omega_{\rm ac}$. $k=0$, i.e. $\Delta_1=\Delta_2=0$, denotes the case where the anti-Stokes optical mode and the acoustic mode are phase-matched with the pump mode. The Langevin noise terms ξ_1 and ξ_2 are the inverse Fourier transform of $\xi_{\rm as}$ and $\xi_{\rm ac}$.

It should be noted that the linearized anti-Stokes Brillouin interaction can be treated as a beam-splitter-like interaction with the excitation (photon or phonon) exchange between the anti-Stokes and acoustic modes at the coupling rate g, as shown in figure 1(c). As the frequency of the optical anti-Stokes field is sufficiently high, the anti-Stokes field sits its quantum ground state and can be seen as equivalent to be coupled to an optical thermal environment at effectively zero temperature. With the excitation exchange, the optical anti-Stokes mode constitutes a source of essentially zero entropy for the acoustic mode and thus extracts the phonons out of the acoustic mode.

3. Steady-state cooling limit

In fact, when the pump power is strong enough, the system enters the strong coupling regime, in which the effective coupling strength exceeds the intrinsic dissipation in either of the anti-Stokes and acoustic modes,

i.e. $g \gg \gamma, \Gamma$. In the following discussion, we focus on the strong coupling regime and consider that optical and acoustic frequency shifts are within the linewidth of the acoustic mode ($\Delta_{1,2} < \Gamma$). Furthermore, for the backward Brillouin scattering in a typical waveguide, the mechanical dissipation is generally far larger than the optical dissipation ($\Gamma \gg \gamma$) and $\Delta_2 \ll \Delta_1$ when $k \neq 0$ because of the slow acoustic group velocity ($v_{ac} \ll v_o$). Therefore, combining the Langevin equation described by equation (2.4) with noise correlations, a set of differential equations for second-order moments $N_a = \langle a^\dagger a \rangle, N_b = \langle b^\dagger b \rangle, \langle a^\dagger b \rangle$ can be obtained (see the supplementary material), where N_b and N_a correspond to the mean phonon and photon numbers. By solving these differential equations, the steady state of the mean phonon number can be expressed as

$$N_b^{ss} \simeq \frac{4g^2(\gamma+\Gamma)+\gamma(\gamma+\Gamma)^2+4\gamma(\Delta_1-\Delta_2)^2}{4g^2(\gamma+\Gamma)+\gamma\Gamma(\gamma+\Gamma)+4\gamma(\Delta_1-\Delta_2)^2\frac{\Gamma}{\gamma+\Gamma}}\frac{\Gamma}{\gamma+\Gamma}n_{th}. \tag{3.1}$$

In the strong coupling regime, we obtain $N_b^{ss} \approx \Gamma/(\gamma+\Gamma)n_{th}$ which is independent of the coupling strength. In the regime, where light waves experience much lower dissipation than acoustic phonons (typical waveguide Brillouin interaction), the phonon heating rate induced by thermal noise exceeds the cooling rate associated to optical dissipation, which largely constrains the phonon cooling factor and gives rise to a fundamental steady-state cooling limit.

4. State swapping under the strong coupling regime

Furthermore, the strong optomechanical interaction generates a high fidelity transfer of quantum states between the anti-Stokes photons and acoustic phonons, i.e. state swapping including swapping heating and swapping cooling. Under the strong coupling regime, the time evolution of the mean phonon number can be described by

$$\begin{aligned} N_b &= N_{b,1} + N_{b,2}, \\ N_{b,1} &\simeq -n_{th}\frac{2(\Gamma-\gamma)g^2-\gamma((\Delta_1-\Delta_2)^2+\gamma\Gamma)}{(\gamma+\Gamma)\Omega^2}e^{-\frac{\gamma+\Gamma}{2}t}+N_b^{ss}, \\ N_{b,2} &\simeq n_{th}\frac{2g^2-\gamma(\gamma+\Gamma)/4}{\Omega^2}e^{-\frac{\gamma+\Gamma}{2}t}\cos(\Omega t) \\ &\quad + n_{th}\frac{\gamma g-\gamma(\gamma+\Gamma)^2/(16g)}{\Omega^2}e^{-\frac{\gamma+\Gamma}{2}t}\sin(\Omega t), \end{aligned} \tag{4.1}$$

where $\Omega = \sqrt{4g^2+2(\Delta_1-\Delta_2)^2-(\Gamma-\gamma)^2/4}$. We note that the phonon occupancy experiences a Rabi oscillation with an exponentially decaying envelope and can be divided into two parts $N_{b,1}$ and $N_{b,2}$. $N_{b,1}$ does not experience oscillation and tends to the steady-state cooling limit N_b^{ss} with an exponentially decaying rate $(\gamma+\Gamma)/2$, which implies effects of optical and mechanical dissipations on phonon occupancy. $N_{b,2}$ exhibits a Rabi oscillation with period $T = 2\pi/\Omega \sim \pi/g$, which reveals the energy transfer between photons and phonons, i.e. swapping heating and cooling processes, in the strong coupling regime.

We show the level diagram of the linearized optomechanical interaction with state swapping in figure 1(d). Solid curves correspond to cooling processes including swapping cooling (A), optical dissipation (C), and mechanical dissipation (D) and dashed curves denote heating processes containing swapping heating (B) and thermal heating (E). We see that two phonon cooling routes exist including the route $A \to C$ and route D where the first route ($A \to C$) is constrained by the optical dissipation process C. In the strong coupling regime while the energy exchanging rate between photons and phonons exceeds the optical dissipation rate, this constrain in the first cooling route will cause a saturation of phonon cooling for a higher coupling strength. This is the reason that the phonon cooling speed, i.e. the exponentially decaying envelope in equation (4.1), and the steady-state cooling limit are independent of the coupling strength g in the strong coupling regime. We present simulation results of time evolution of the phonon occupancy $N_b(t)$ with different coupling strength g in figure 2(a). Here, we choose the thermal phonon occupation $n_{th} = 1000$ without loss of generality, since the Brillouin frequency for the backward Brillouin scattering in a typical waveguide reaches the GHz-level. It confirms that the strong optomechanical coupling does not generate a faster cooling speed and a significant lower steady-state cooling limit comparing with the weak coupling when the optical dissipation is far smaller than the mechanical dissipation.

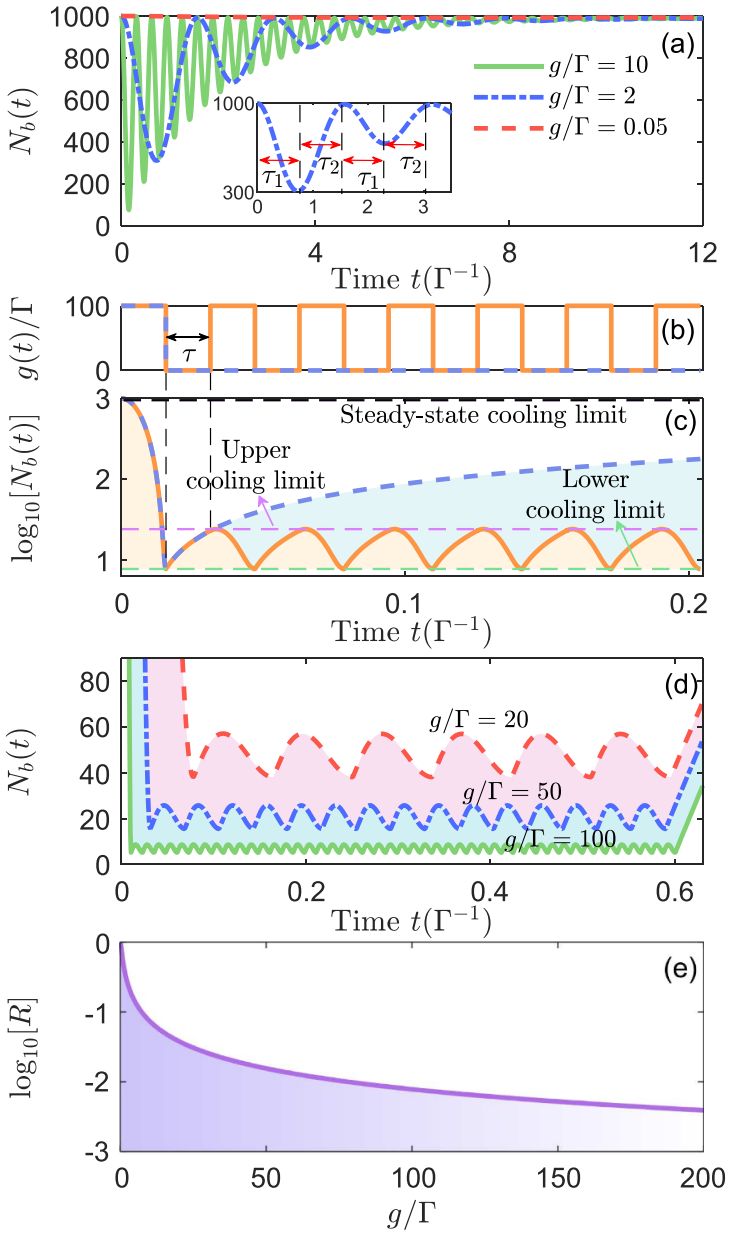

Figure 2. (a) Time evolution of mean phonon number $N_b(t)$ for $g/\Gamma = 0.05, 2, 10$ where the inset shows the initial transient process of $N_b(t)$ for the case $g/\Gamma = 2$. (b) shows the dynamical modulation of $g(t)$ and (c) describes the corresponding time evolution of $N_b(t)$, where blue dashed (orange solid) curves denote the single pulse (periodic pulse) modulation, where τ is the pump switch-off time. (d) Time evolution of $N_b(t)$ under pulse modulation of the coupling strength with different intensities, where $\tau = 0.05T$. (e) Brillouin cooling factor R versus the coupling strength. Other parameters are $\gamma/\Gamma = 0.01$, $\Delta_1/\Gamma = 0.3$, $\Delta_2/\Gamma = 3 \times 10^{-5}$, and $n_{\rm th} = 1000$.

5. Dynamic Brillouin cooling via pulsed modulation

5.1. Breaking the steady-state cooling limit

Although the strong optomechanical interaction does not considerably contribute to the steady-state cooling limit, it results in a Rabi oscillation for the phonon occupancy and thus leads the minimum phonon occupancy to be far smaller than the steady-state cooling limit, as shown in figure 2(a). The system transfers from state $|n, m\rangle$ to state $|n, m-1\rangle$ by extracting phonons out of the acoustic mode during the swapping-cooling-dominant time period τ_1, as shown in the inset of figure 2(a). Analogously, it transfers from $|n, m\rangle$ to $|n, m+1\rangle$ by generating phonons during the swapping-heating-dominant time period τ_2. These two time periods alternate with a cycle $\tau_1 = \tau_2 = T/2$. To break the steady-state cooling limit and obtain a significant cooling rate, here we dynamically modulate the coupling strength $g(t)$ through a pulsed pump laser to continuously permit the swapping-cooling-dominant process and suppress the swapping-heating-dominant process. We consider a short enough Brillouin-active waveguide [65], i.e.

$L \ll v_o T/2$, where light fields will quickly pass through the waveguide and thus a pump laser can generate a time-varying coupling strength with the pulsed shape by switching on and off the pump, as shown in figure 1(b). We switch on the pump laser during the swapping-cooling-dominant time periods (τ_1) to strengthen phonon absorption and switch off the pump during the swapping-heating-dominant time periods (τ_2) to halt the reversible Rabi oscillation and thus suppress the swapping heating process.

We illustrate the modulation scheme of the pulsed coupling strength and the corresponding time evolution of the phonon occupancy in figures 2(b) and (c), respectively. Since the phonon occupancy reaches the minimum value at the end of the first half Rabi oscillation, we switch off the pump abruptly at this time to prevent the energy from transferring back to phonons. During the pump switch-off time period, the phonons are only driven by the thermal environment, thus the phonon occupancy increases with the exponential growing rate $\Gamma/2$. After the optical fields passe through the waveguide, i.e. optical fields are initialized to the vacuum state, we switch on the pump laser to excite the swapping cooling process to absorb phonons and prevent the phonon occupancy from increasing continuously. By periodically modulating the coupling strength to initialize optical fields regularly, we can continuously suppress the swapping and thermal heating processes to keep a low phonon occupancy with a small-amplitude fluctuation and thus break the steady-state cooling limit, as shown by orange solid curves in figures 2(b) and (c). The instantaneous-state cooling limit, i.e. the lower cooling limit (green dashed line) in figure 2(c), can be expressed as

$$N_b^{\mathrm{ins}} \approx \frac{\pi(\Gamma+\gamma)g + (\Delta_1-\Delta_2)^2 - \frac{(\Gamma-\gamma)^2}{4}}{4g^2 + (\Delta_1-\Delta_2)^2 - \frac{(\Gamma-\gamma)^2}{4}} \cdot \frac{\Gamma}{\gamma+\Gamma} n_{\mathrm{th}}. \tag{5.1}$$

In the strong coupling regime, we obtain $N_b^{\mathrm{ins}} \approx \pi(\Gamma+\gamma)N_b^{\mathrm{ss}}/(4g)$, which reduces the Brillouin steady-state cooling limit by a factor of $\pi\Gamma/(4g)$. The upper cooling limit in figure 2(c) can be approximately expressed as $N_b^{\mathrm{upp}} \approx (1+\pi)(\Gamma+\gamma)N_b^{\mathrm{ss}}/(4g)$. We know that in cavity optomechanical systems in the weak coupling regime, the cooling limit in the resolved-sideband regime is mainly dependent on the effective coupling strength G and the optical dissipation rate γ [82, 83], i.e. $\sim n_{\mathrm{th}}G^2/\gamma$. Here, as we consider the strong coupling regime and higher mechanical dissipation and periodically evacuate the photons, the instantaneous-state cooling limit is decided by the ratio between the mechanical dissipation rate and the effective coupling strength.

In fact, the small-amplitude fluctuation around the instantaneous-state cooling limit is induced by the pulse modulation of the coupling strength and the strong optomechanical interaction, which can be optimized by tuning the pump switch-off time τ. In figure 2(d), we show the time evolution of the phonon occupancy with periodical modulation of the coupling strength while the pump switch-off time is $\tau = 0.05T$, where g denotes the intensity of the coupling strength during the pump switch-on time periods. We also present the Brillouin cooling factor R, which is the ratio of the instantaneous cooling limit to the initial phonon occupancy, in figure 2(e). It indicates that a great Brillouin cooling factor, which reduces the steady-state cooling limit ($R \approx 1$) by several orders of magnitude, can be achieved through pulse modulation of the optomechanical interaction, while photons experience lower damping than phonons.

5.2. Optomechanical continuum cooling

Different from the single mode cooling methods in cavity optomechanical systems [10] or the multimode cooling methods in other extended optomechanical systems with many degrees of freedom [30–33], here we can achieve significant phonon cooling over a continuum of acoustic states, i.e. optomechanical continuum cooling with a outstanding bandwidth. We show the simulation results of the optomechanical continuum cooling with different coupling strength g under pulse modulation in figure 3(a), where g describes the intensity of the coupling strength during the pump switch-on time period. We can see that the stronger coupling strength is, the broader bandwidth for the cooled phonons can be achieved. It should be noted that here we only cool a group of phonons within a broad bandwidth from the thermal reservoir, instead of trying to cool the whole mechanical reservoir.

5.3. Switchability of the modulation

In figures 2(b) and (c), we apply the pulse modulation to the coupling strength at the end of the first half Rabi oscillation in order to quickly reach the instantaneous-state cooling limit. Actually, we can exert the pulse modulation at any time and finally cool the phonons to the instantaneous-state cooling limit. This means that this modulation scheme is switchable, as shown in figures 3(b) and (c). The system will reach the instantaneous-state cooling limit when we turn on the modulation and tend to the steady-state cooling limit while we turn off the modulation.

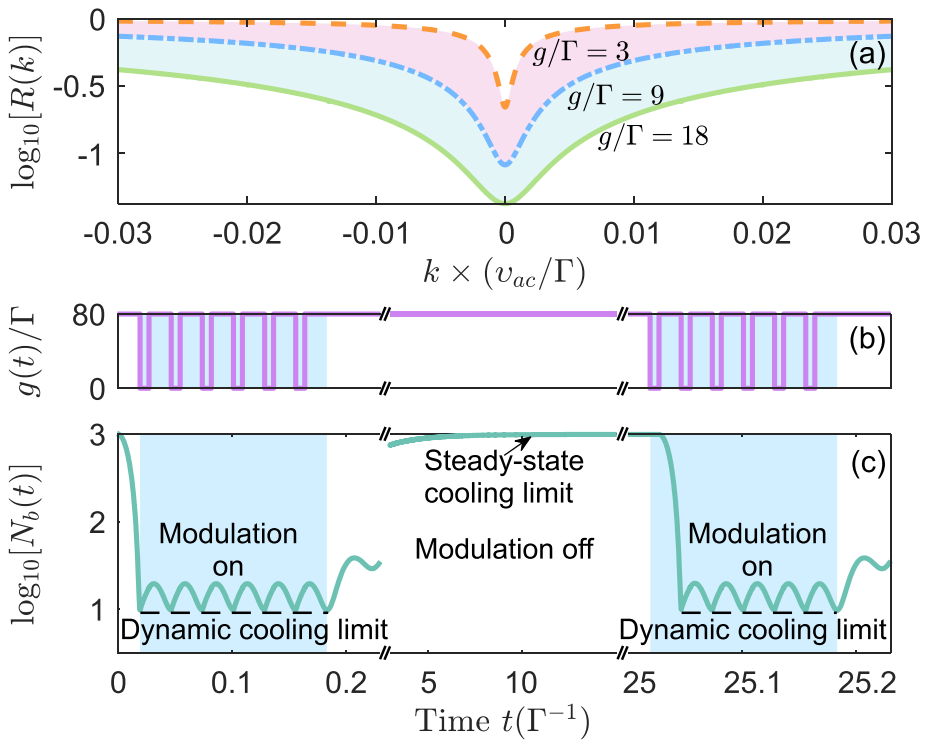

Figure 3. (a) Optomechanical continuum cooling factor R for $g/\Gamma = 3, 9, 18$. (b) and (c) present the switchable modulation scheme of the coupling strength and the corresponding phonon occupancy $N_b(t)$, respectively, where the pump switch-off time $\tau = 0.2T$ and the light blue areas denote the time periods with the modulation turned on.

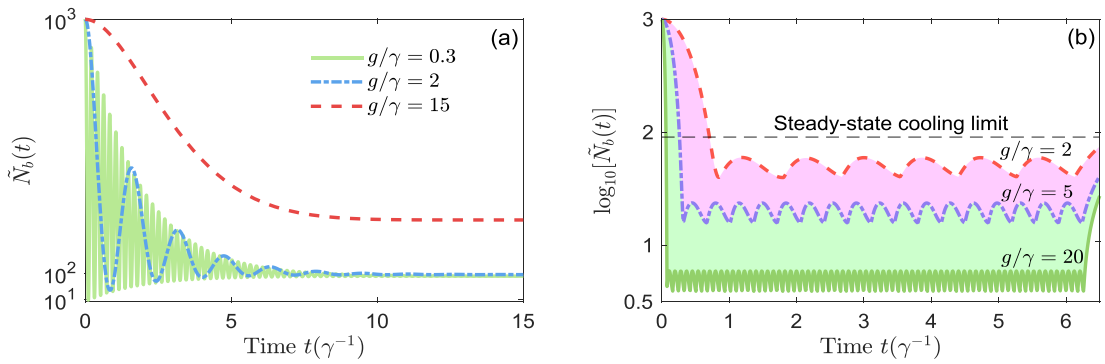

Figure 4. Dynamical Brillouin cooling produced by the forward anti-Stokes intermodal scattering in continuous optomechanical systems. (a) Time evolution of mean phonon number $\tilde{N}_b(t)$ for different coupling strength $g/\gamma = 0.3, 2, 15$. (b) Dynamical Brillouin cooling via pulsed modulation of the coupling intensity. Other parameters are $\Gamma/\gamma = 0.1$, $\Delta_1/\gamma = 0.05$, $\Delta_2/\gamma = 5 \times 10^{-6}$, and $n_{\rm th} = 1000$.

6. Dynamic cooling generated by forward Brillouin interaction

In fact, the above modulation scheme can be also applied to the optomechanical cooling generated by the forward anti-Stokes intermodal Brillouin scattering in continuous systems [55], where the mechanical dissipation is lower than the optical dissipation. Actually, like the backward scattering case stated above, the phonon occupancy $\tilde{N}_b(t)$ corresponding to the forward intermodal Brillouin scattering exhibits a Rabi oscillation in the strong coupling regime, which enables lower phonon occupancy at some instantaneous states, as shown in figure 4(a). Here, we choose the ratio between mechanical and optical dissipations according to the parameters measured in experiment [55]. With a pulsed modulation of the optomechanical interaction in the strong coupling regime to enhance the swapping cooling process while suppressing the swapping heating process, the phonon occupancy can be continuously maintained in a lower occupation with a small-amplitude fluctuation, which breaks the steady-state cooling limit, as shown in figure 4(b).

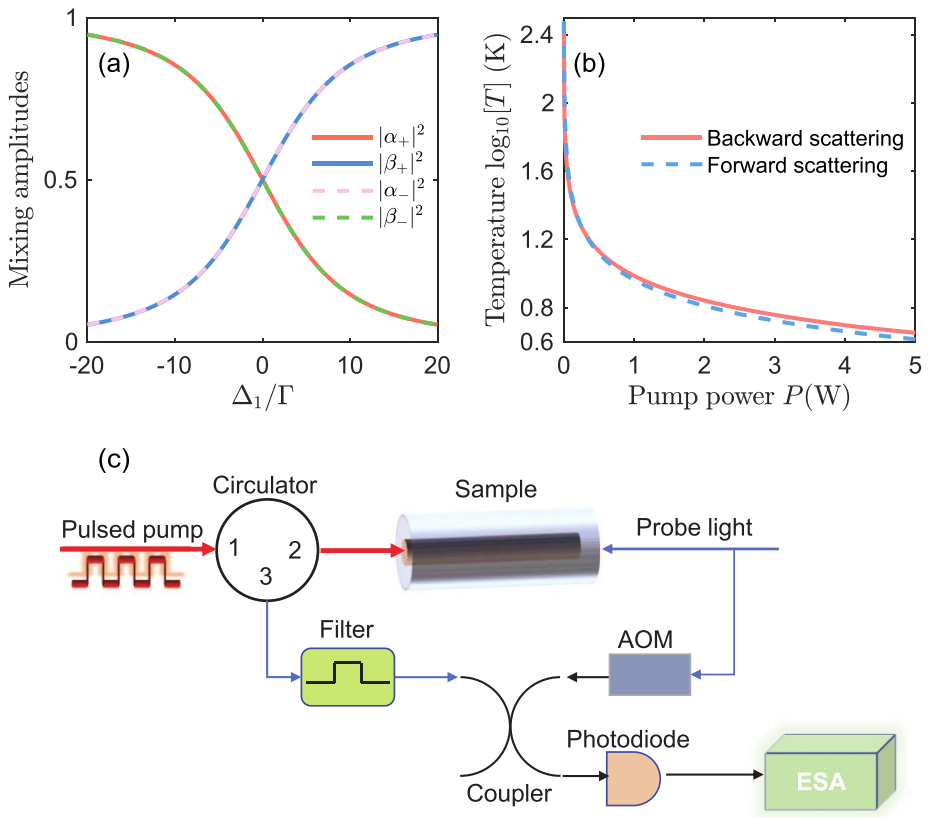

Figure 5. (a) Mixing amplitudes $|\alpha_\pm|^2, |\beta_\pm|^2$ versus Δ_1. (b) Temperature T of the cooled phonons versus pump power, where the red-solid (blue-dashed) curve denotes the cooled temperature induced by backward (forward) Brillouin anti-Stokes scattering. (c) Schematic diagram of the experimental setup for cooling via backward Brillouin scattering.

7. Discussion

In fact, our dynamic cooling scheme contains two processes, which includes a coherent and reversible process during the pump switching on time period and an incoherent and irreversible process during the pump switching off time period. By modulating the two processes via a pulsed pump, we can greatly enhance the energy transfer from phonons to photons and largely suppress the reverse process. Furthermore, the coherent and reversible process originates from the strong correlation between anti-Stokes photons and acoustic phonons in the strong coupling regime, which can be explained by introducing the concept of polariton operators as discussed in [84]. By diagonalizing the coefficient matrix in equation (2.4), we introduce polariton operators as follows

$$\Psi_+ = \alpha_+ a + \beta_+ b, \quad \Psi_- = \alpha_- a + \beta_- b, \tag{7.1}$$

which correspond to the coherent superposition of the anti-Stokes photons and acoustic phonons. The normalized coherent mixing amplitudes, i.e. $|\alpha_\pm|^2 + |\beta_\pm| = 1$, describe the correlation between photons and phonons. We show the mixing amplitudes $|\alpha_\pm|^2, |\beta_\pm|^2$ with different Δ_1 in figure 5(a). It can be seen that the polariton operators are close to half phononic and half photonic, i.e. $|\alpha_\pm|^2 = |\beta_\pm|^2 \approx 1/2$, near the phase-matching point ($\Delta_1 \approx 0$), which shows a great mixing of anti-Stokes photons and acoustic phonons and implies the strong photon–phonon correlation. This significant photon–phonon mixing induces the swapping heating and cooling processes.

In addition, a lot of integrated waveguides with high Brillouin gain have been reported recently [65]. A significant cooling factor can be obtained by applying the dynamic modulation scheme to these small waveguides with length of cm level. For example [85], reported a 5.8 cm long integrated waveguide, where the Brillouin gain is 750 $\mathrm{m}^{-1}\,\mathrm{W}^{-1}$, Brillouin frequency is 7.6 GHz, and Brillouin linewidth is 40 MHz. By applying our dynamic modulation scheme to this waveguide, we show the effective temperature of the cooled phonons via backward anti-Stokes Brillouin scattering in figure 5(b) (see the red-solid curve). It implies that the temperature of phonons can be cooled down to around 4.5 K from room temperature 300 K. This means that by using a pulsed pump with pulse width of ∼0.7 ns and peak power of ∼5 W, the phonon occupation can be cooled to around 12 phonons at room temperature. A schematic of the experimental setup is provided

in figure 5(c). [55] presents a phonon cooling of 30 K at room temperature in a 2.3 cm long waveguide by using forward intermodal anti-Stokes Brillouin scattering, where the Brillouin gain, Brillouin frequency, Brillouin linewidth, and optical loss rate are 470 $m^{-1} W^{-1}$, 6 GHz, 14 MHz, and 180 MHz, respectively. However, by applying a pulsed pump with pulse width of ∼2 ns and peak power of ∼5 W, the phonons can be cooled down to ∼4 K from room temperature, i.e. with a phonon occupation around 14, as shown by the blue-dashed curve in figure 5(b). Although the cooled phonons presented in figure 5(b) do not reach the ground state, it exhibits the potential of our dynamic cooling scheme for studying macroscopic quantum effects at high temperature in the continuous optomechanical systems. Actually, if we apply our dynamic cooling scheme to the waveguide reported in [85] at an environment temperature of 20 K, the acoustic phonons can be cooled down to the quantum ground state with a phonon occupation lower than 1. Furthermore, if the Brillouin linewidth and the Brillouin gain of the integrated waveguide in [85] can be improved to 0.2 MHz and 1000 $m^{-1} W^{-1}$, it is possible to cool the acoustic phonons down to the ground state with a phonon occupation of ∼0.7 at room temperature by using a pulsed pump with pulse width of ∼8.7 ns and peak power of ∼5 W.

8. Conclusions

We have shown that by periodically modulating the Brillouin interaction with a pulsed pump in the strong coupling regime, we can stimulate the swapping cooling process while suppressing the swapping heating process and thus obtain a significant Brillouin cooling factor with several orders of magnitude. It proves that cooling traveling-wave phonons into quantum ground state by utilizing backward Brillouin scattering is possible in continuous optomechanical systems while mechanical dissipation exceeds optical dissipation. In addition, this pulse modulation scheme can be switchable. Distinct from other pulsed cooling schemes that use complicated control methods [75, 86] or dynamic dissipative cooling by exploiting the optical dissipation [76] in cavity optomechanical systems, the simplicity and convenience of our method is achieved by simply controlling the pump pulse, which makes the dynamic cooling scheme an effective experimental tool for quantum optomechanics. Moreover, our scheme can also be applied to Brillouin cooling produced by forward intermodal Brillouin scattering and break the steady-state cooling limit. It should be pointed out that even though there is a small-amplitude fluctuation of the phonon occupancy around the instantaneous-state cooling limit, the Brillouin cooling limit can be viewed as stable in the sense of time averaging while the time scale is larger than the Rabi oscillation cycle T [76]. This work opens the way for the exploration of quantum phenomena in continuous optomechanical systems through backward Brillouin scattering. The dynamical control of optomechanical interaction also provides a new way to study quantum technologies, ranging from mechanical quantum states generation, quantum information processing, and high-precise measurement.

Data availability statement

We have provided comprehensive derivations in the supplementary material and presented the analytical solutions for our main results in this theoretical work. So we believe that the simulation codes that we used to obtain the simulation results and plot these figures shown in our work are not important to understand our work. Of course, if readers are interested in these codes and detail simulation data, they can contact us and ask for them. The data that support the findings of this study are available upon reasonable request from the authors.

Acknowledgment

The authors would like to acknowledge very useful discussions with Christian Wolff, Claudiu Genes, Florian Marquardt, and Yu-xi Liu. This work is supported by the Max-Planck-Society through the independent Max Planck Research Groups Scheme.

ORCID iDs

Changlong Zhu https://orcid.org/0000-0003-1979-3381
Birgit Stiller https://orcid.org/0000-0002-9868-9998

References

[1] LaHaye M D, Buu O, Camarota B and Schwab K C 2004 Approaching the quantum limit of a nanomechanical resonator *Science* **304** 74

[2] Teufel J D, Donner T, Castellanos-Beltran M A, Harlow J W and Lehnert K W 2009 Nanomechanical motion measured with an imprecision below that at the standard quantum limit *Nat. Nanotechnol.* **4** 820
[3] Purdy T P, Peterson R W and Regal C A 2013 Observation of radiation pressure shot noise on a macroscopic object *Science* **339** 801
[4] Palomaki T A, Teufel J D, Simmonds R W and Lehnert K W 2013 Entangling mechanical motion with microwave fields *Science* **342** 710
[5] Riedinger R, Wallucks A, Marinković I, Löschnauer C, Aspelmeyer M, Hong S and Gröblacher S 2018 Remote quantum entanglement between two micromechanical oscillators *Nature* **556** 473
[6] Ockeloen-Korppi C F, Damskägg E, Pirkkalainen J M, Asjad M, Clerk A A, Massel F, Woolley M J and Sillanpää M A 2018 Stabilized entanglement of massive mechanical oscillators *Nature* **556** 478
[7] Marshall W, Simon C, Penrose R and Bouwmeester D 2003 Towards quantum superpositions of a mirror *Phys. Rev. Lett.* **91** 130401
[8] Pikovski I, Vanner M R, Aspelmeyer M, Kim M S and Brukner Č 2012 Probing Planck-scale physics with quantum optics *Nat. Phys.* **8** 393
[9] Arndt M and Hornberger K 2014 Testing the limits of quantum mechanical superpositions *Nat. Phys.* **10** 271
[10] Aspelmeyer M, Kippenberg T J and Marquardt F 2014 Cavity optomechanics *Rev. Mod. Phys.* **86** 1391
[11] Marquardt F, Chen J P, Clerk A A and Girvin S M 2007 Quantum theory of cavity-assisted sideband cooling of mechanical motion *Phys. Rev. Lett.* **99** 093902
[12] Teufel J D, Donner T, Li D, Harlow J H, Allman M S, Cicak K, Sirois A J, Whittaker J D, Lehnert K W and Simmonds R W 2011 Sideband cooling of micromechanical motion to the quantum ground state *Nature* **475** 395
[13] Chan J, Mayer Alegre T P, Safavi-Naeini A H, Hill J T, Krause A, Gröblacher S, Aspelmeyer M and Painter O 2011 Laser cooling of a nanomechanical oscillator into its quantum ground state *Nature* **478** 89
[14] Qiu L, Shomroni I, Seidler P and Kippenberg T J 2020 Laser cooling of a nanomechannical oscillator to its zero-point energy *Phys. Rev. Lett.* **124** 173601
[15] Riedinger R, Hong S, Norte R A, Slater J A, Shang J, Krause A G, Anant V, Aspelmeyer M and Gröblacher S 2016 Non-classical correlation between single photons and phonons from a mechanical oscillator *Nature* **530** 313
[16] Hong S, Riedinger R, Marinković I, Wallucks A, Hofer S G, Norte R A, Aspelmeyer M and Gröblacher S 2017 Hanbury brown and twiss interferometry of single phonons from an optomechanical resonator *Science* **358** 203
[17] Marinković I, Wallucks A, Riedinger R, Hong S, Aspelmeyer M and Gröblacher S 2018 Optomechanical bell test *Phys. Rev. Lett.* **121** 220404
[18] Barzanjeh S, Pirandola S, Vitali D and Fink J M 2020 Microwave quantum illumination using a digital receiver *Sci. Adv.* **6** eabb0451
[19] Fiaschi N, Hensen B, Wallucks A, Benevides R, Li J, Mayer Alegre T P and Gröblacher S 2021 Optomechanical quantum teleportation *Nat. Photon.* **15** 817
[20] Scharnhorst N, Cerrillo J, Kramer J, Leroux I D, Wübbena J B, Retzker A and Schmidt P O 2018 Experimental and theoretical investigation of a multimode cooling scheme using multiple electromagnetically-induced-transparency resonances *Phys. Rev.* A **98** 023424
[21] Huang J, Lai D G, Liu C, Huang J F, Nori F and Liao J Q 2022 Multimode optomechanical cooling via general dark-mode control *Phys. Rev.* A **106** 013526
[22] Sommer C and Genes C 2019 Partial optomechanical refrigeration via multimode cold-damping feedback *Phys. Rev. Lett.* **123** 203605
[23] Sommer C, Ghosh A and Genes C 2020 Multimode cold-damping optomechanics with delayed feedback *Phys. Rev.* A **2** 033299
[24] Lai D G, Huang J, Hou B P, Nori F and Liao J Q 2021 Domino cooling of a coupled mechanical-resonator chain via cold-damping feedback *Phys. Rev.* A **103** 063509
[25] Lai D G, Huang J F, Yin X L, Hou B P, Li W, Vitali D, Nori F and Liao J Q 2020 Nonreciprocal ground-state cooling of multiple mechanical resonators *Phys. Rev.* A **102** 011502(R)
[26] Naseem M T and Müstecaplıoğlu O E 2021 Ground-state cooling of mechanical resonators by quantum reservoir engineering *Commun. Phys.* **4** 95
[27] Bhattacharya M and Meystre P 2008 Multiple membrane cavity optomechanics *Phys. Rev.* A **78** 041801(R)
[28] Xu X-W, Zhao Y-J and Liu Y-X 2013 Entangled-state engineering of vibrational modes in a multimembrane optomechanical system *Phys. Rev.* A **88** 022325
[29] Lee D, Underwood M, Mason D, Shkarin A B, Hoch S W and Harris J G E 2015 Multimode optomechanical dynamics in a cavity with avoided crossings *Nat. Commun.* **6** 6232
[30] Spethmann N, Kohler J, Schreppler S, Buchmann L and Stamper-Kurn D M 2016 Cavity-mediated coupling of mechanical oscillators limited by quantum back-action *Nat. Phys.* **12** 27
[31] Ockeloen-Korppi C F, Damskägg E, Pirkkalainen J-M, Asjad M, Clerk A A, Massel F, Woolley M J and Sillanpää M A 2018 Stabilized entanglement of massive mechanical oscillators *Nature* **556** 478
[32] Heinrich G, Ludwig M, Qian J, Kubala B and Marquardt F 2011 Collective dynamics in optomechanical arrays *Phys. Rev. Lett.* **107** 043603
[33] Xuereb A, Genes C and Dantan A 2012 Strong coupling and long-range collective interactions in optomechanical arrays *Phys. Rev. Lett.* **109** 223601
[34] Zhang M, Shah S, Cardenas J and Lipson M 2015 Synchronization and phase noise reduction in micromechanical oscillator arrays coupled through light *Phys. Rev. Lett.* **115** 163902
[35] Gärtner C, Moura J P, Haaxman W, Norte R A and Gröblacher S 2018 Integrated optomechanical arrays of two high reflectivity SiN membranes *Nano Lett.* **18** 7171
[36] Ren H, Shah T, Pfeifer H, Brendel C, Peano V, Marquardt F and Painter O 2022 Topological phonon transport in an optomechanical system *Nat. Commun.* **13** 3476
[37] de Jong M, Li J, Gärtner C, Norte R and Groblacher S 2022 Coherent mechanical noise cancellation and cooperativity competition in optomechanical arrays *Optica* **9** 170
[38] Delić U, Reisenbauer M, Dare K, Grass D, Vuletić V, Kiesel N and Aspelmeyer M 2020 Cooling of a levitated nanoparticle to the motional quantum ground state *Science* **367** 892
[39] Dania L, Heidegger K, Bykov D S, Gerchiari G, Araneda G and Northup T E 2022 Position measurement of a levitated nanoparticle via interference with its mirror image *Phys. Rev. Lett.* **129** 013601
[40] Fang K, Matheny M H, Luan X and Painter O 2016 Optical transduction and routing of microwave phonons in cavity-optomechanical circuits *Nat. Photon.* **10** 489

[41] Patel R N, Wang Z, Jiang W, Sarabalis C J, Hill J T and Safavi-Naeini A H 2018 Single-mode phononic wire *Phys. Rev. Lett.* **121** 040501
[42] Van Laer R, Baets R and Van Thourhout D 2016 Unifying Brillouin scattering and cavity optomechanics *Phys. Rev.* A **93** 053828
[43] Rakich P and Marquardt F 2018 Quantum theory of continuum optomechanics *New. J. Phys.* **20** 045005
[44] Shuman E S, Barry J F and DeMille D 2010 Laser cooling of a diatomic molecule *Nature* **467** 820
[45] Zhelyazkova V, Cournol A, Wall T E, Matsushima A, Hudson J J, Hinds E A, Tarbutt M R and Sauer B E 2014 Laser cooling and slowing of CaF molecules *Phys. Rev.* A **89** 053416
[46] Sommer C, Joly N Y, Ritsch H and Genes C 2019 Laser refrigeration of gas filled hollow-core fibres *AIP Adv.* **9** 105213
[47] Rayner A, Heckenberg N R and Rubinsztein-Dunlop H 2003 Condensed-phase optical refrigeration *J. Opt. Soc. Am.* B **20** 1037
[48] Sheik-Bahae M and Epstein R I 2007 Optical refrigeration *Nat. Photon.* **1** 693
[49] Sheik-Bahae M and Epstein R I 2009 Laser cooling of solids *Laser Photon. Rev.* **3** 67
[50] Seletskiy D V, Melgaard S D, Bigotta S, Di Lieto A, Tonelli M and Sheik-Bahae M 2010 Laser cooling of solids to cryogenic temperatures *Nat. Photon.* **4** 161
[51] Knall J, Vigneron P B, Engholm M, Dragic P, Yu N, Ballato J, Bernier M and Digonnet M J F 2020 Laser cooling in a silica optical fiber at atmospheric pressure *Opt. Lett.* **45** 1092
[52] Knall J, Engholm M, Ballato J, Dragic P, Yu N and Digonnet M J F 2020 Experimental comparison of silica fibers for laser cooling *Opt. Lett.* **45** 4020
[53] Chen Y-C, Kim S and Bahl G 2016 Brillouin cooling in a linear waveguide *New J. Phys.* **18** 115004
[54] Huy K P, Godet A, Sylvestre T and Beugnot J-C 2017 Brillouin phonon cooling by electro-optic feedback (arXiv:1708.09220)
[55] Otterstrom N T, Behunin R O, Kittlaus E A and Rakich P T 2018 Optomechanical cooling in a continuous system *Phys. Rev.* X **8** 041034
[56] Zoubi H and Hammerer K 2017 Quantum nonlinear optics in optomechanical nanoscale waveguides *Phys. Rev. Lett.* **119** 123602
[57] O'Brien J L 2007 Optical quantum computing *Science* **318** 1567
[58] Fowler A G, Mariantoni M, Martinis J M and Cleland A N 2012 Surface codes: towards practical large-scale quantum computation *Phys. Rev.* A **86** 032324
[59] Habraken S J M, Stannigel K, Lukin M D, Zoller P and Rabl P 2012 Continuou mode cooling and phonon routers for phononic quantum networks *New J. Phys.* **14** 115004
[60] Vermersch B, Guimond P-O, Pichler H and Zoller P 2017 Quantum state transfer via noisy photonic and phononic waveguides *Phys. Rev. Lett.* **118** 133601
[61] Kuzyk M C and Wang H 2018 Scaling phononic quantum networks of solid-state spins with closed mechanical subsystems *Phys. Rev.* X **8** 041027
[62] Tomes M, Marquardt F, Bahl G and Carmon T 2011 Quantum-mechanical theory of optomechanical Brillouin cooling *Phys. Rev.* A **84** 063806
[63] Bahl G, Tomes M, Marquardt F and Carmon T 2012 Observation of spontaneous Brillouin cooling *Nat. Phys.* **8** 203
[64] Agarwal G S and Jha S S 2013 Multimode phonon cooling via three-wave parametric interactions with optical fields *Phys. Rev.* A **88** 013815
[65] Eggleton B J, Poulton C G, Rakich P T, Steel M J and Bahl G 2019 Brillouin integrated photonics *Nat. Photon.* **13** 664
[66] Koehler J R, Noskov R E, Sukhorukov A A, Novoa D, St P Russell J 2017 Coherent control of flexural vibrations in dual-nanoweb fibers using phase-modulated two-frequency light *Phys. Rev.* A **96** 063822
[67] Noskov R E, Koehler J R and Sukhorukov A A 2018 Interply of cascaded Raman- and Brillouin-like scattering in nanostructured optical waveguides *ACS Photonics* **5** 1074
[68] Merklein M, Stiller B, Vu K, Madden S J and Eggleton B J 2017 A chip-integrated coherent photonic-phononic memory *Nat. Commun.* **8** 574
[69] Huy K P, Beugnot J C, Tchahame J C and Sylvestre T 2016 Strong coupling between phonons and optical beating in backward Brillouin scattering *Phys. Rev.* A **94** 043847
[70] Verhagen E, Deléglise S, Weis S, Schliesser A and Kippenberg T J 2012 Quantum-coherent coupling of a mechanical oscillator to an optical cavity mode *Nature* **482** 63
[71] Safavi-Naeini A H, Thourhout D V, Baets R and Laer R V 2019 Controlling phonons and photons at the wavelength scale: integrated photonics meets integrated phononics *Optica* **6** 213
[72] Hensinger W K, Utami D W, Goan H S, Schwab K, Monroe C and Milburn G J 2005 Ion trap transducers for quantum electromechanical oscillators *Phys. Rev.* A **72** 041405(R)
[73] Tian L, Allman M S and Simmonds R W 2008 Parametric cooling between macroscopic quantum resonators *New J. Phys.* **10** 115001
[74] Tian L and Wang H L 2010 Optical wavelength conversion of quantum states with optomechanics *Phys. Rev.* A **82** 053806
[75] Wang X T, Vinjanampathy S, Strauch F W and Jacobs K 2011 Ultraefficient cooling of resonators: beating sideband cooling with quantum control *Phys. Rev. Lett.* **107** 177204
[76] Liu Y C, Xiao Y F, Luan X S and Wong C W 2013 Dynamical dissipative cooling of a mechanical resonator in strong coupling optomechanics *Phys. Rev. Lett.* **110** 153606
[77] Kharel P, Behunin R O, Renninger W H and Rakich P T 2016 Noise and dynamics in forward Brillouin interactions *Phys. Rev.* A **93** 063806
[78] Boyd R W, Rzazewski K and Narum P 1990 Noise initiation of stimulated Brillouin scattering *Phys. Rev.* A **42** 5514
[79] Pagani M, Chan E H W and Minasian R A 2014 A Study of the linearity Performance of a stimulated Brillouin Scattering-Based microwave photonic bandpass filter *J. Lightwave Technol.* **32** 999
[80] Sipe J E and Steel M J 2016 A Hamiltonian treatment of stimulated Brillouin scattering in nanoscale integrated waveguides *New. J. Phys.* **18** 045004
[81] Zoubi H and Hammerer K 2016 Optomechanical multimode hamiltonian for nanophotonic waveguides *Phys. Rev.* A **94** 053827
[82] Genes C, Vitali D, Tombesi P, Gigan S and Aspelmeyer M 2008 Ground-state cooling of a micromechanical oscillator: comparing cold damping and cavity-assisted cooling schemes *Phys. Rev.* A **77** 033804
[83] Wilson-Rae I, Nooshi N, Zwerger W and Kippenberg T J 2007 Theory of ground state cooling of a mechanical oscillator using dynamical backaction *Phys. Rev. Lett.* **99** 093901
[84] Zoubi H 2018 Phonon-polaritons in nanoscale waveguides *J. Opt.* **20** 095001
[85] Morrison B *et al* 2017 Compact Brillouin devices through hybrid integration on silicon *Optica* **4** 847
[86] Machnes S, Cerrillo J, Aspelmeyer M, Wieczorek W, Plenio M B and Retzker A 2012 Pulsed laser cooling for cavity optomechanical resonators *Phys. Rev. Lett.* **108** 153601